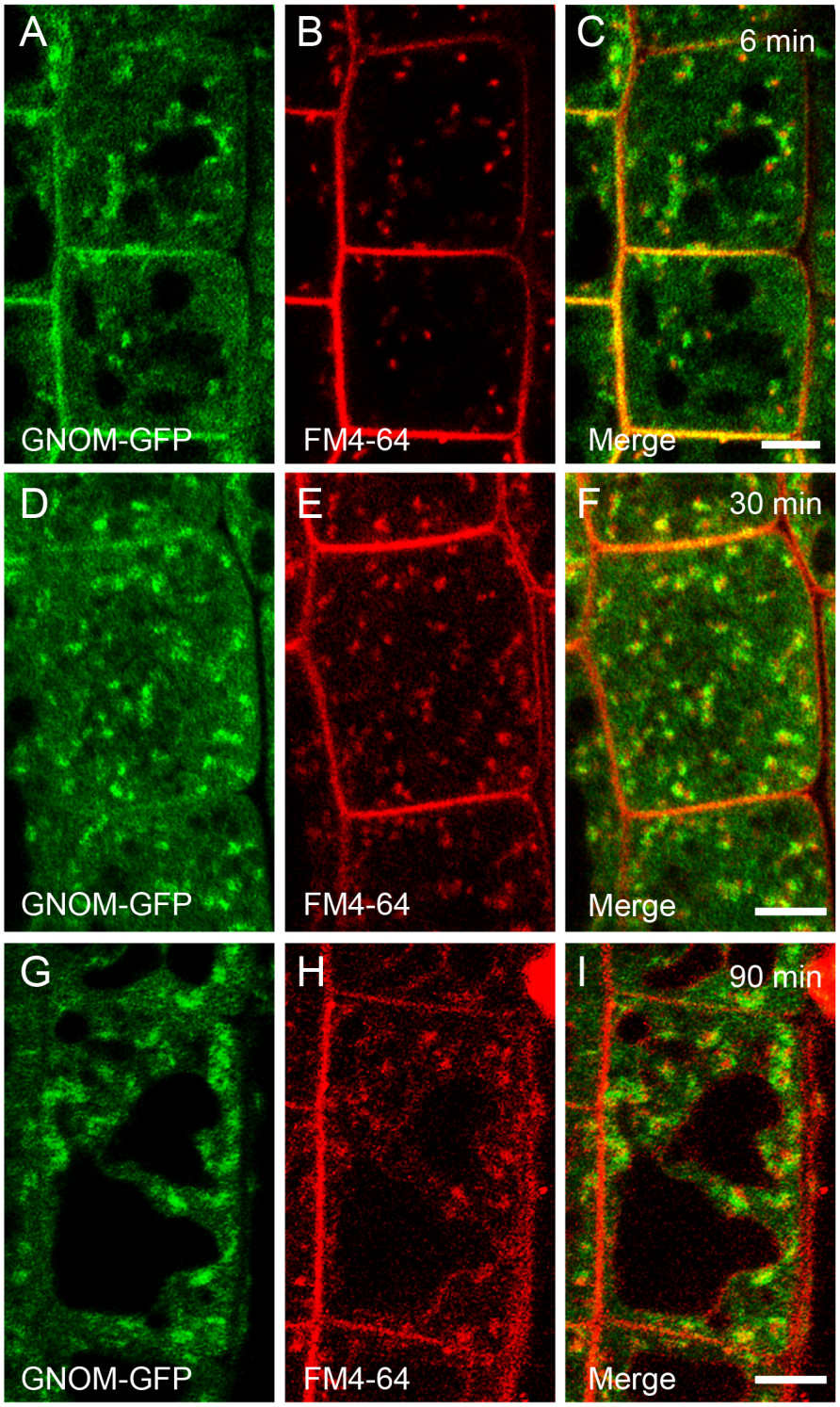

Supplemental Figure 1. GNOM-GFP is less efficiently stained by the endocytosis tracer FM4-64.

(A) to **(I)** Double-labeling of GNOM-GFP (green) and FM4-64 (red) in root epidermal cells. Subcellular localization of GNOM-GFP [**(A)**, **(D)**, and **(G)**], FM4-64 [**(B)**, **(E)**, and **(H)**], and their merged images [**(C)**, **(F)**, and **(I)**] are shown. Incubation times with FM4-64 are indicated on the merged image.

Bars = 3 μm.

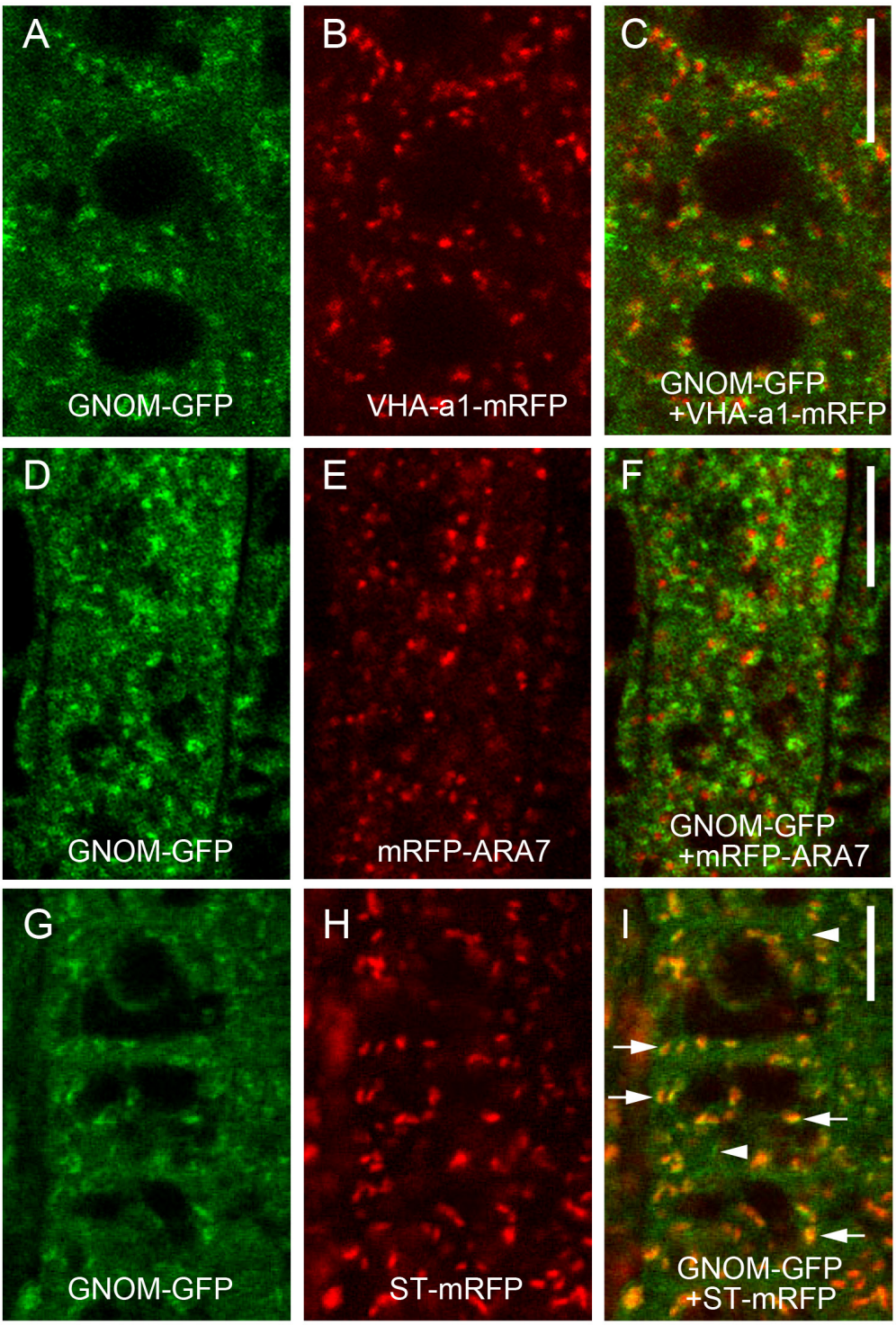

Supplemental Figure 2. The distribution of GNOM-GFP and RFP-tagged organelle markers. **(A)** to **(I)** Double-labeling of GNOM-GFP (green) and RFP-tagged organelle markers (red) in root epidermal cells. GNOM-GFP does not colocalize with VHA-a1-mRFP-labeled [**(A)** to **(C)**] or mRFP-ARA7-labeled [**(D)** to **(F)**] organelles, whereas GNOM-GFP strongly colocalizes with ST-mRFP-labeled Golgi apparatus [**(G)** to **(I)**]. Arrows and arrowheads indicate ST-mRFP-positive and -negative GNOM-GFP-labelled compartments, respectively.

Bars = 8 μm.

Supplemental Data. Naramoto et al. Plant Cell (2014) 10.1105/tpc.114.125880

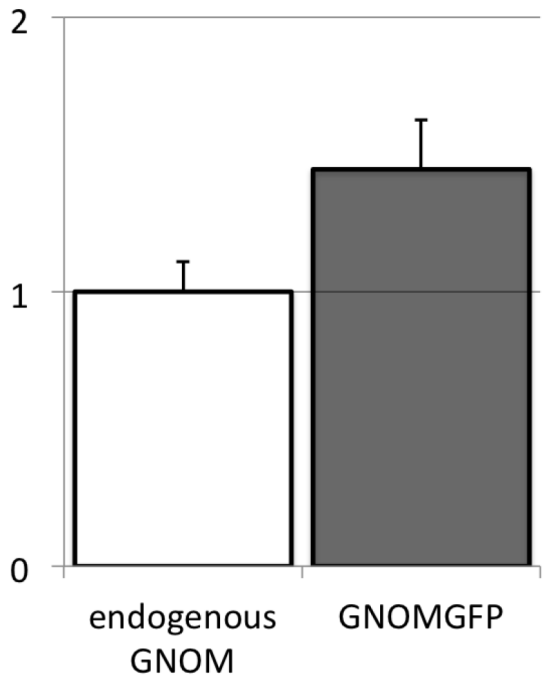

Supplemental Figure 3. Quantitative RT-PCR analysis of GNOM-GFP expression

Relative expression of levels of GNOM-GFP in pGNOM::GNOM:GFP seedlings and endogenous GNOM in wild-type seedlings. Total RNA isolated from 5 days old seedlings were used for the analysis. Transcript levels were measured using real-time RT-PCR. The mean level of GNOM mRNA in Columbia was taken as a standard (1.0). Error bars indicate the SD values for data from three independent experiments.

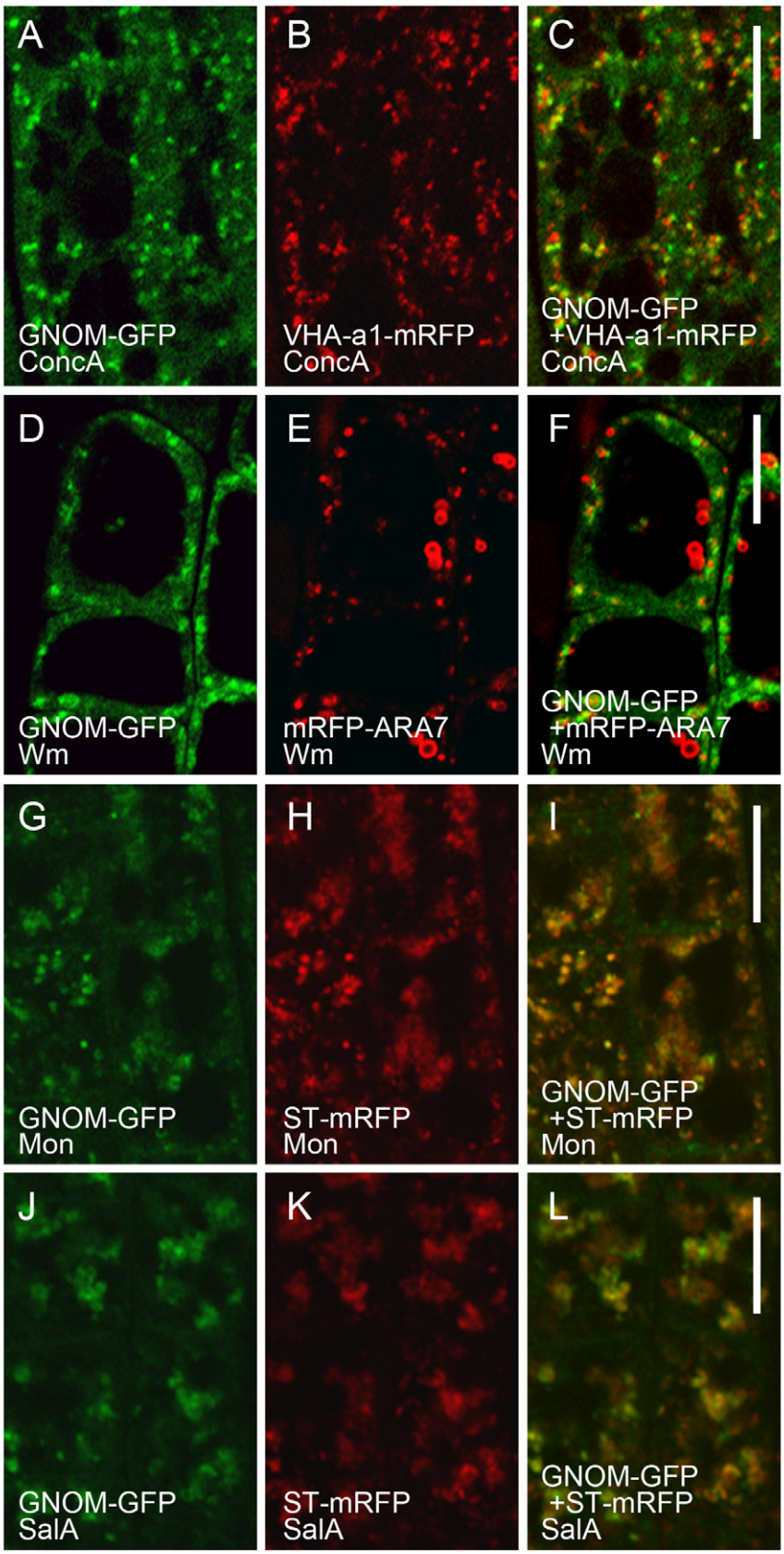

Supplemental Figure 4. The distribution of GNOM-GFP and RFP-tagged organelle markers in response to pharmacological interference

(A) to **(C)** Double-labeling of GNOM-GFP and VHA-a1-mRFP in root epidermal cells in the presence of ConcA.

(D) to **(F)** Root epidermal cells co-expressing GNOM-GFP and mRFP-ARA7 after the treatment with Wm.

(G) to **(L)** Double-labeling of GNOM-GFP and ST-mRFP in root epidermal cells treated with Mon [**(G)** to **(I)**] and SalA [**(J)** to **(L)**].

Bars = 8 μm.

Supplemental Data. Naramoto et al. Plant Cell (2014) 10.1105/tpc.114.125880

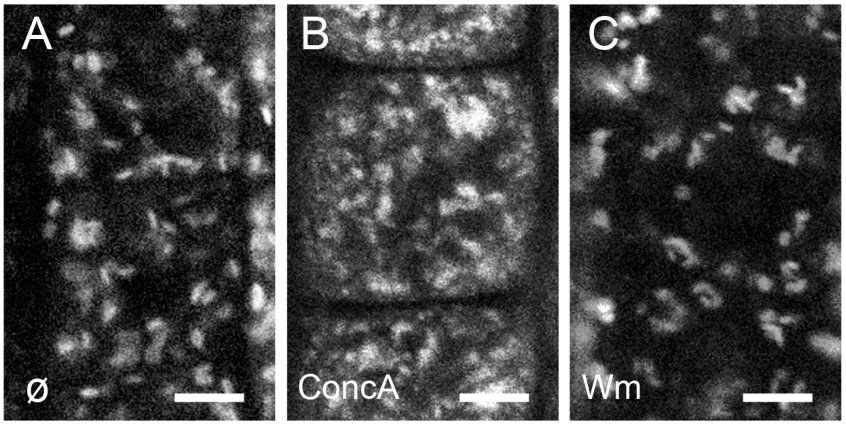

Supplemental Figure 5. The distribution of ST-mRFP is not strongly affected by concanamycin and wortmannin.

(A) to **(C)** Root cells expressing ST-mRFP after no treatment **(A)**, after treatment with ConcA **(B)**, and after treatment with Wm **(C)**. Treatment with ConcA and Wm was performed for 1hr.

Bars = 4 μm.

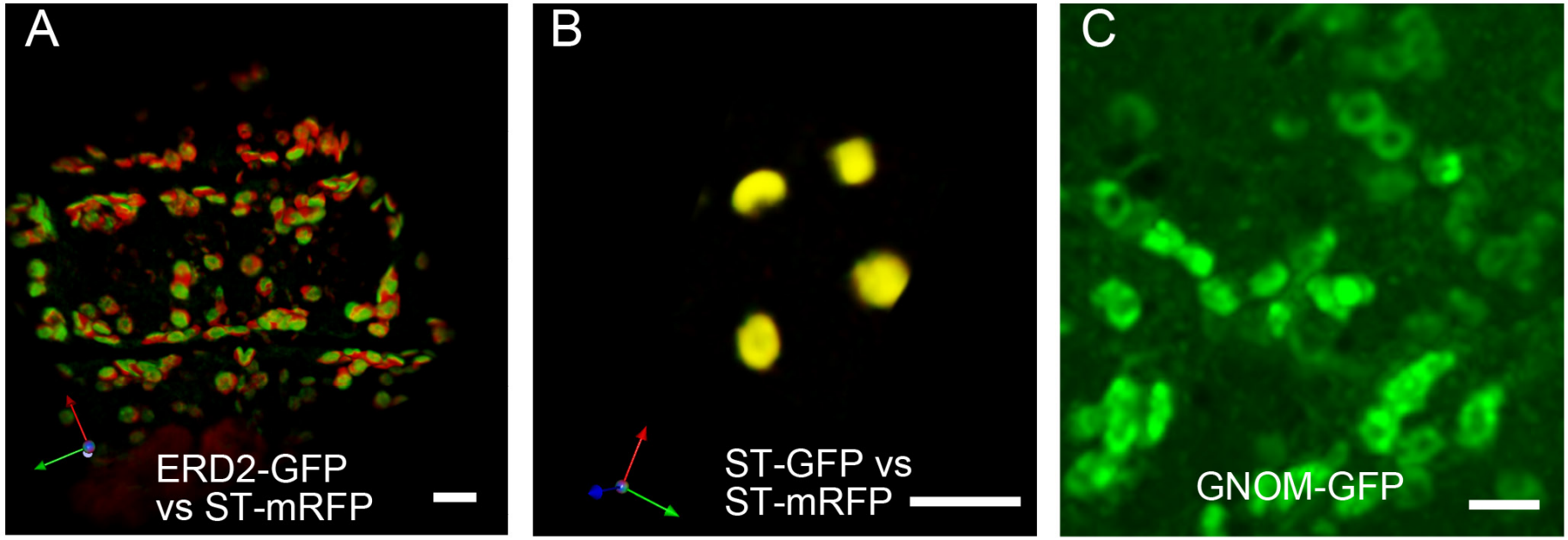

Supplemental Figure 6. High resolution microscopy observation systems succeeded in observing the plant Golgi apparatus.

(A) 3D image of the *cis*-Golgi marker, ERD2-GFP (green), and the *trans*-Golgi marker ST-mRFP (red). A merged image is shown in **(A)**. Note the clear separation of cis- and trans-Golgi cisternae.

(B) Double-labeling of ST-GFP (green) and ST-mRFP (red). A merged 3D image is shown in **(B)**. Note essentially complete colocalization.

(C) Extended focus image of GNOM-GFP. GNOM-GFP displays ring-like localization.

Bars = 2μm.

Supplemental Data. Naramoto et al. Plant Cell (2014) 10.1105/tpc.114.125880

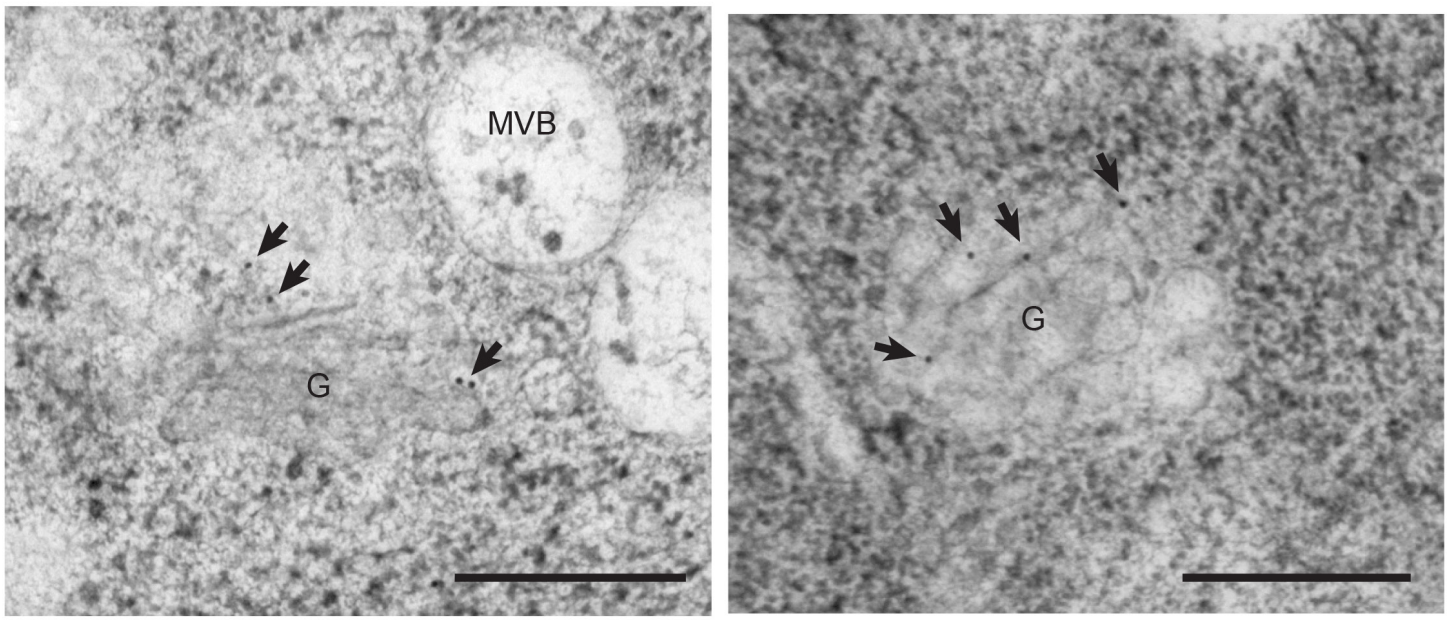

Supplemental Figure 7. GNOM-GFP localizes to the Golgi apparatus in BFA-untreated root cells. Series of IEM pictures showing GNOM-GFP. Note that GNOM-GFP tends to localize to the periphery of Golgi cisternae. The golgi apparatus and multi vesicular body is designated as "G" and "MVB" , respectively. Arrows indicate the localization of gold particles. Bars = 500 nm.

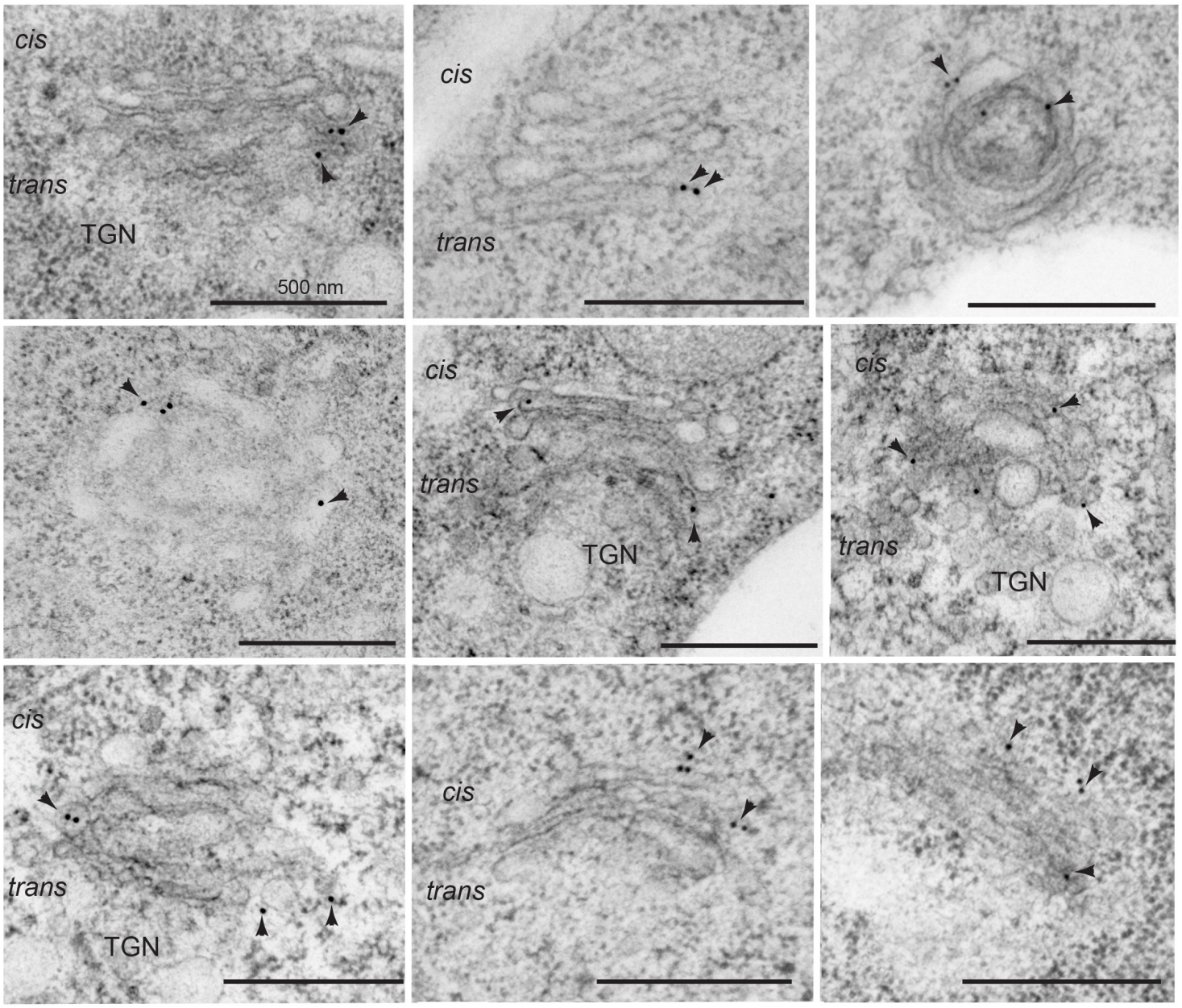

Supplemental Figure 8. GNOM-GFP localizes to the Golgi apparatus in BFA-treated root cells. Series of IEM pictures showing GNOM-GFP. Note that GNOM-GFP tends to localize to the periphery of Golgi cisternae. *cis* Golgi cisternae and *trans* Golgi cisternae are designated as "*cis*" and "*trans*", respectively. Arrowheads indicate the localization of gold particles. Bars = 500 nm.

Supplemental Data. Naramoto et al. Plant Cell (2014) 10.1105/tpc.114.125880

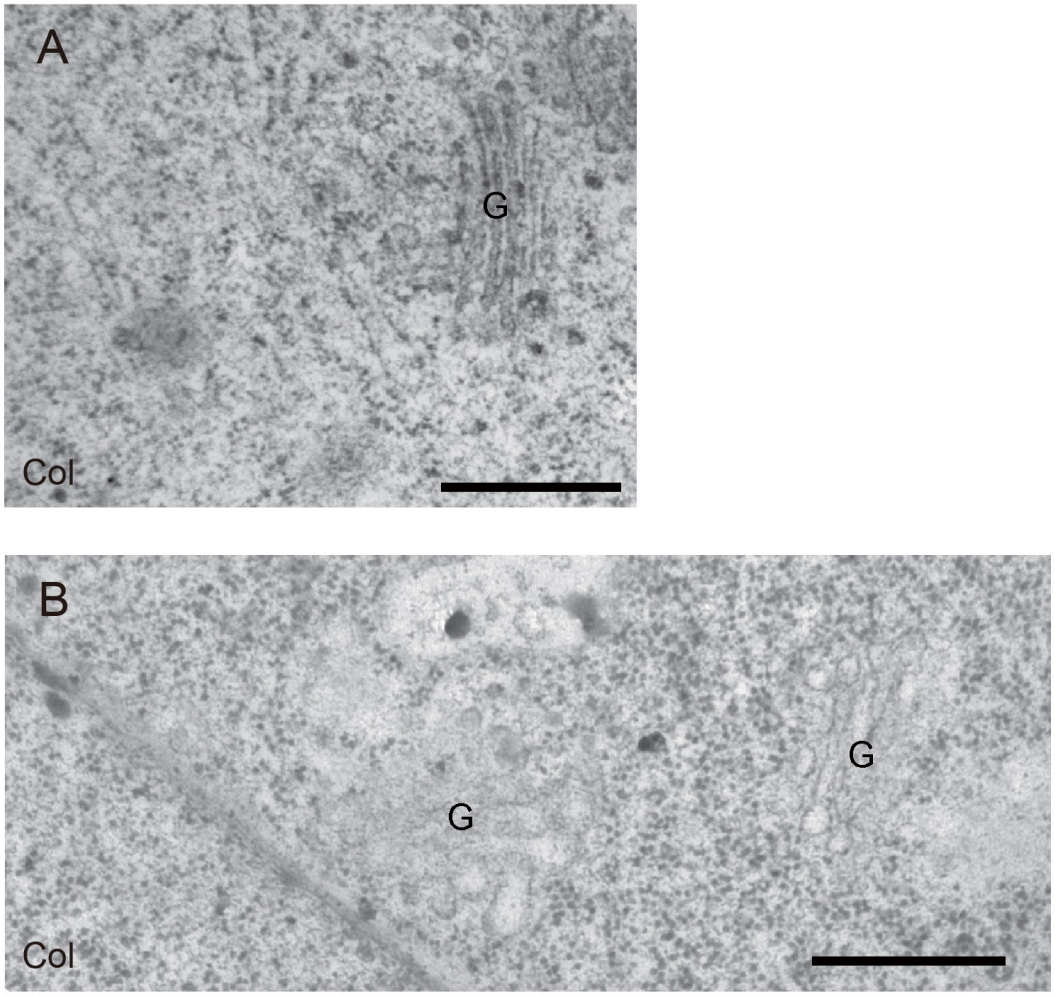

Supplemental Figure 9. An anti-GFP antibody does not stain the Golgi apparatus.
(A) and **(B)** Negative controls for IEM analysis of GNOM-GFP. No signals are detected at the Golgi apparatus in either untreated **(A)** or BFA–treated **(B)** wild-type seedlings when using the anti-GFP antibody. The Golgi apparatus is designated as “G” within the figure. Bars = 500 nm.

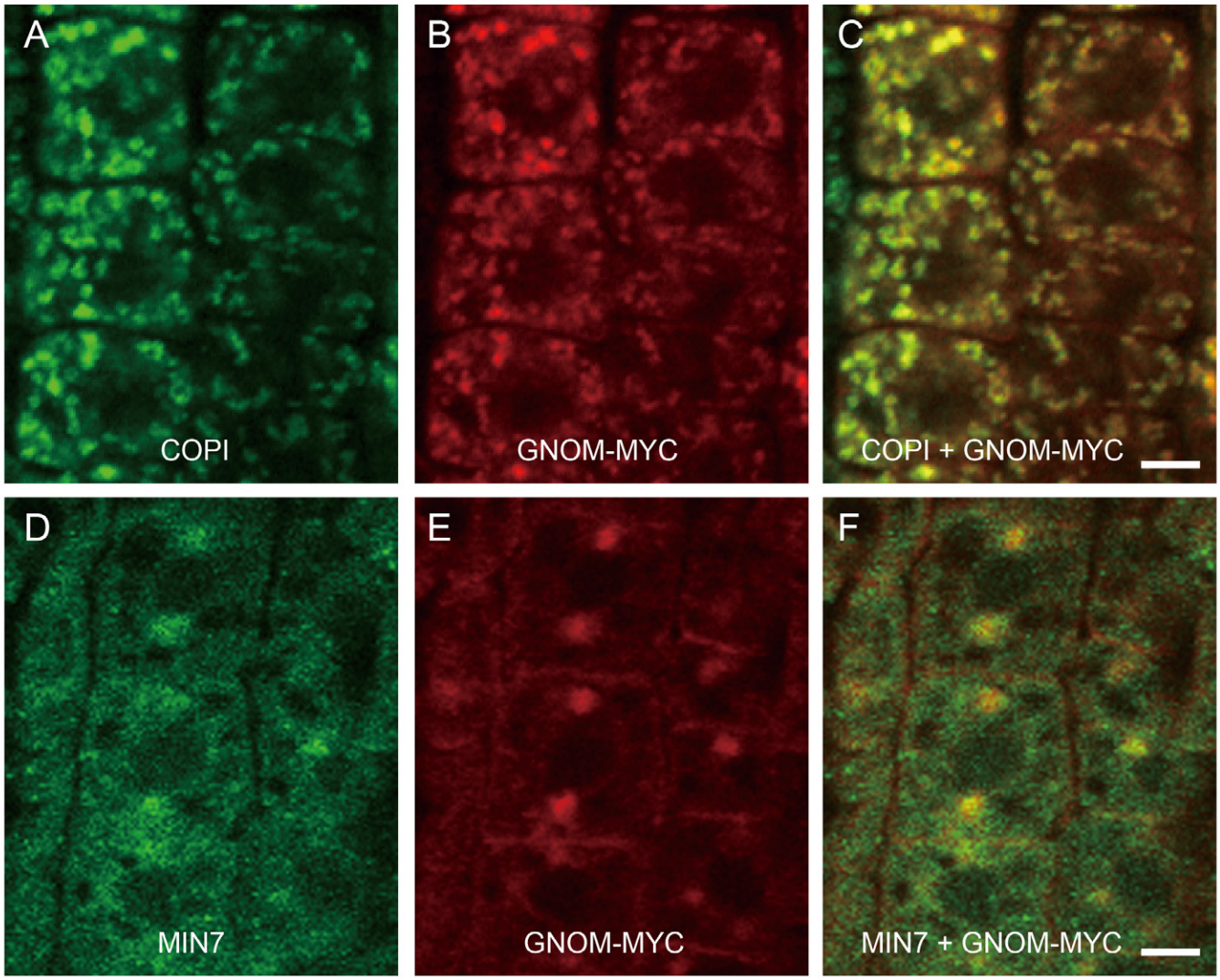

Supplemental Figure 10. GNOM-MYC is stabilized at the Golgi apparatus during short-time BFA treatment, and subsequently localizes at the TGN during mid-term BFA treatment.

(A) to **(C)** Double-labeling of functional BFA-sensitive GNOM-MYC (red) and anti-COPI antibody by treatment with 50 μM BFA for 5 min. The anti-COPI antibody Golgi marker **(A)** colocalizes with functional GNOM-MYC **(B)**. A merged image is shown in **(C)**.

(D) to **(F)** Double-labeling of functional BFA-sensitive GNOM-MYC (red) and anti-MIN7 antibody (green) by treatment with 50 μM BFA for 1 hr. Although GNOM-MYC localizes at the Golgi apparatus shortly after the start of BFA treatment, GNOM-MYC **(E)** localizes at MIN7-labeled TGN **(D)** after BFA treatment for 1hr. A merged image is shown in **(F)**.

Bars = 4μm.

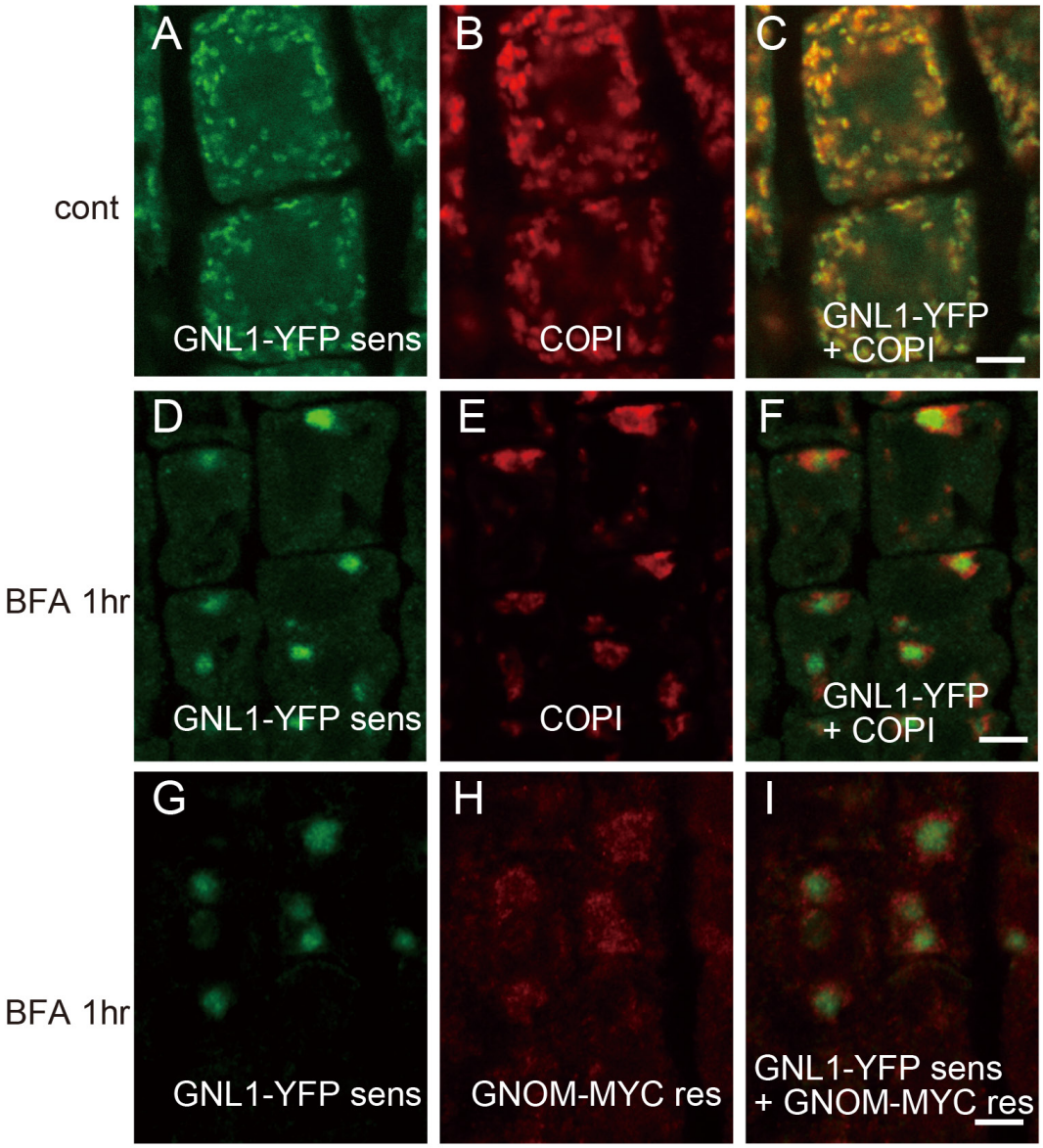

Supplemental Figure 11. Engineered BFA-sensitive functional GNL1-YFP translocates from the Golgi apparatus to endosomes following BFA treatment.

(A) to **(I)** Subcellular localization analysis of Arabidopsis root cells that co-express engineered BFA-sensitive GNL1-YFP and engineered BFA-resistant GNOM-MYC. Engineered BFA-sensitive GNL1-YFP **(A)** localizes to the anti-COPI antibody-labeled Golgi apparatus **(B)** under normal conditions. A merged image is shown in **(C)**.

By contrast, BFA-sensitive GNL1-YFP [**(D)** and **(G)**] does not localize to the Golgi apparatus labeled by the anti-COPI antibody **(E)** or BFA-resistant GNOM-MYC **(H)** following BFA treatment. Merged images are shown in **(F)** and **(I)**, respectively. Note that the engineered BFA-resistant GNOM-MYC **(H)** appears to remain at the Golgi apparatus even after BFA treatment.

Bars = 3 μm.

Supplemental Data. Naramoto et al. Plant Cell (2014) 10.1105/tpc.114.125880

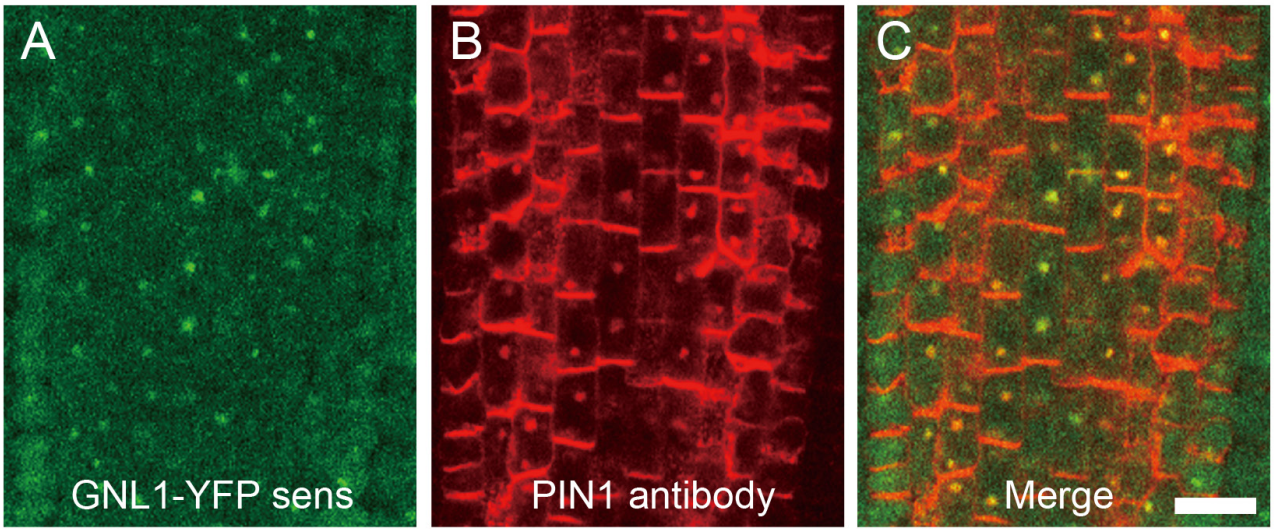

Supplemental Figure 12. PIN1 is internalized by the inhibition of GNL1 function. **(A)** to **(C)** Double-labeling of BFA-treated gnl1emb30 root cells co-expressing GNL1 BFA-sensitive YFP and GNOM BFA-resistant MYC with GNL1-YFP (green) and the PIN1 antibody (red). GNL1-YFP **(A)** and the anti-PIN1 antibody **(B)** are colocalized at the BFA body **(C)** by treatment with 50 μM BFA for 1hr.
Note PIN1 internalization, suggesting inhibited recycling.
Bar =10 μm.

Supplemental Data. Naramoto et al. Plant Cell (2014) 10.1105/tpc.114.125880

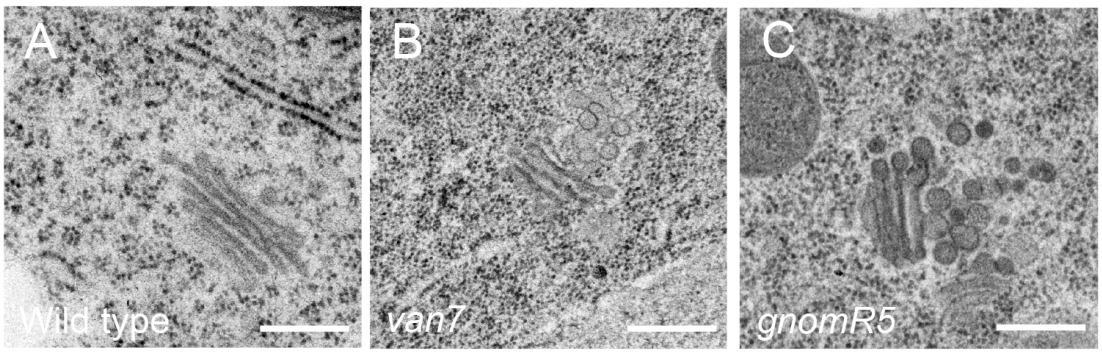

Supplemental Figure 13. TGN structure is malformed in *van7* and *gnomR5* mutants.

(A) to **(C)** EM images of wild-type **(A)**, *van7* mutant **(B)**, and *gnomR5* mutant **(C)** root cells. Note that the TGN is highly vesiculated in *gnom* mutant cells.

Bars = 250 nm.